Acta Mechanica 179, 11–23 (2005)
DOI 10.1007/s00707-005-0248-9

Acta Mechanica
Printed in Austria

Heat transfer enhancement of nanofluids in rotary blade coupling of four-wheel-drive vehicles

S.-C. Tzeng, C.-W. Lin, and **K. D. Huang,** Chang Hua, Taiwan, R.O.C.

Received December 2, 2004; revised 9 March, 2005
Published online: June 20, 2005

Summary. This study adds CuO and Al_2O_3 nano particles and antifoam respectively into cooling engine oil. A comparison is made between their heat transfer performance and that of oil without adding such substances. The experimental platform is a real-time four-wheel-drive (4WD) transmisson system. It adopts advanced rotary blade coupling (RBC), where a high local temperature occurs easily at high rotating speed. Therefore, it is imperative to improve the heat transfer efficiency. Any resolution to such problems requires a thorough understanding of the thermal behavior of the rotating flow field within the power transmission system. The experiment measures the temperature distribution of RBC exterior at four different rotating speeds (400rpm, 800rpm, 1200rpm and 1600rpm), simulating the conditions of a real car at different rotating speeds and investigating the optimum possible compositions of a nanofluid for higher heat transfer performance.

Nomenclature

$\vec{a}$	acceleration
$\vec{F}$	body force
k_f	fluid thermal conductivity, W/m°C
Nu	Nusselt number $(= 2q_{in}r_i/(T_w - T_\infty)k_f)$
P	pressure
q_{in}	heat input, W/m^2
r_i	inner radius, m
r_o	outer radius, m
r_m	mean radius, m $(= (r_o + r_i)/2)$
$\vec{r}$	particle's position
T	temperature, °C
Ta	Taylor number $(= \Omega^2 r_m (r_o - r_i)^3/\nu^2)$
t	time
$\vec{V}$	particle's velocity

Greek symbol

δ	deviation of the Nu vs. Ta correlation, seen in Table 2
Φ	scalar function, seen in Eq. (5)
Ω	angular speed (rad/s)
μ	dynamic viscosity
ρ	fluid density
ν	kinematic viscosity
ξ	vorticity

Subscripts

o	hydrostatic condition
w	wall
∞	surrounding

Superscripts

$'$	variation quantity

1 Introduction

With the rapid development of the automobile industry and the improvement of living standards, the automobile, a traditional transportation means, now plays an increasing sport and recreational role and the demand for all-terrain four-wheel-drive (4WD) vehicles is booming. The development of 4WD vehicles has experienced full time and part time driving. It was not until recently that real time 4WD technology became available. It combines the features of sedans and those of 4WD off-road vehicles, adopting forward wheel drive (FWD) on smooth roads and 4WD on rugged roads and slippery roads. All the power transmission can be automatically performed instantly [1], [2].

The present power transmission system of advanced 4WD vehicles is RBC, which drives the vehicle by its forward wheels on smooth roads to achieve better operating performance and save fuel, and is capable of transmitting power to the rear wheels instantly and without human interference as forward wheels have a rotating difference on rugged roads to prevent skidding. The design of RBC is so precise that its rotating components may be damaged by excessive thermal stress if the local high temperature is higher than 266°F. The system malfunction may prevent the power from being transmitted to the rear wheels, consequently severely affecting the vehicle performance. Moreover, the RBC is irreparable and any damage requires replacement altogether, which is very costly. Therefore, the development of highly efficient cooling technology to contain the excessive thermal stress on the components of the power transmission system has become an important problem in the research on heat transfer.

Generally, the heat transfer performance of solid metals is far better than that of liquids. At room temperature, the thermal conductivity of copper is about 700 times higher than water, and 3000 times higher than cooling oil. It is evident that adding suspending solid metal particles into a liquid can dramatically enhance the heat transferring performance of liquid. Maxwell [3] theoretically predicted that the addition of suspending round particles could effectively enhance heat transfer efficiency about 100 years ago. The test for industrial application, which was performed by Liu and others [4] in 1998, covered the effects of particle size, volume, and flow rate upon heat transfer. However, the particles in the test were all reckoned by millimeter and micron and, as they moved with the liquid within tubes, they easily jammed and wore them. In 1995, Choi [5] first proposed to call a liquid containing nano-particles nanofluid. This means adding suspended nanocrystalline particles into such liquids as water or oil. Recent research findings showed that the characteristics of particles whose size is less than 100nm are much different from those of previous millimeter and micron sizes. The nano size of metal particles makes them more like liquid atoms moving, enhancing liquid stability instead of jamming tubes. As far as heat transfer performance is concerned, as the volume of the occupied channel is fixed, 10nm particles, whose surface area per volume is 1000 times bigger than that of 10μm particles, are more propitious in terms of heat conduction and heat convection.

Eastman et al. [6] found that, under experimental conditions, adding CuO nano particles into water at different ratios could dramatically enhance heat transfer performance. For example, adding 4% CuO nano particles improved the heat transferring efficiency by 50%. Furthermore, there was no deposit in the liquid although the densities of metal particles and liquid were different. These findings showed that nano metal particles are very compatible with liquids and no separation occurs. The research made by Lee and his team [7] revealed that a nanofluid could obviously enhance heat transfer. According to their test, the heat transferring efficiency of a nanofluid containing 4.3% Al_2O_3 was increased by 30%. This is because not only metal particles on nano level increase their surface area, but their characteristics are also very close to those of the liquid. More stable performance and enhanced heat transfer can be provided by mixing them up with lubricant. Wang and Xu [8] adopted steady-state plating in measuring the heat transfer efficiency of nanofluids in their research on the heat transfer performance of nanofluids. They mixed CuO and Al_2O_3 with water, engine oil, and glycerin to make nanofluids. Their experiments proved that the heat transfer efficiency of nanofluids was evidently higher than that of traditional liquids without adding nano metal particles. Based on relevant experimental results, they established some empirical formulas about heat transfer performance, which were very helpful for related workers. Keblinski et al. [9] in 2001 explored the relationship between the size of the particles and the heat transfer performance of liquid. They proved that the heat transfer efficiency increased as the size of the particles decreased. The transfer of heat would be very fast as the size reached the nano level thanks to the charge distribution of nano atoms.

Lubricant nanofluid could not only improve lubricant performance, but also decrease friction. Some researchers have many fruitful findings in this field. Li et al. [10] conducted experiments on lubricant nanofluids containing powdered IrO_2 and ZrO_2 of nano structure and found that the friction on the surface of 100C6 steel was remarkably improved. Under microstructural analysis, the lubricant nanofluids had excellent performance. Therefore, this team held that nanofluid could effectively decrease friction.

To make the experimental conditions match the real operation as close as possible, apart from taking the Ro–number and actual geometrical parameters, the real RBC of a power transmission system of a real-time 4WD vehicle is adopted. The research subject of cooling characteristics is the power transmission system of actual parameters and sizes. The test would provide reference to the actual engineering design. Apart from measuring overall heat transferring coefficients, local heat transferring coefficients are also measured to understand the effects of local high temperature on the blades.

2 Theoretical analysis

The acceleration of moving particles in the rotating flow field can be expressed as

$$\vec{a} = \frac{d\vec{V}}{dt} = \frac{\partial^2 \vec{r}}{\partial t^2} + 2\left(\vec{\Omega} \times \frac{\partial \vec{r}}{\partial t}\right) + \left(\frac{\partial \vec{\Omega}}{\partial t} \times \vec{r}\right) + \vec{\Omega} \times (\vec{\Omega} \times \vec{V}) + \vec{a}_o, \tag{1}$$

where $\vec{a_o} \equiv \frac{d\vec{V_o}}{dt}$. $\vec{\Omega} \times (\vec{\Omega} \times \vec{\mathrm{V}})$ in Eq. (1) is the centripetal acceleration, and $2(\vec{\Omega} \times \frac{\partial \vec{r}}{\partial t})$ is the Corolis acceleration.

As for a Newtonian fluid, its momentum conservation can be expressed in vector mode as

$$\rho \frac{D\vec{V}}{Dt} = -\nabla P + \rho \vec{F} + \mu \nabla^2 \vec{V} + \frac{\mu}{3} \nabla(\nabla \cdot \vec{V}). \tag{2}$$

Assuming $\nabla \cdot \vec{V} = 0$ under incompressible flow condition, Eq. (2) can be simplified as

$$\frac{D\vec{V}}{Dt} = -\frac{1}{\rho}\nabla P + \vec{F} + v\nabla^2 \vec{V}, \tag{3}$$

where, taking no account of the body force, it can be deduced from Eqs. (1) and (3) that

$$\frac{D\vec{V}}{Dt} + 2(\vec{\Omega} \times \vec{V}) + \left[\left(\vec{\Omega} \times (\vec{\Omega} \times \vec{r})\right) + A_o\right] = -\frac{1}{\rho}\nabla P + v\nabla^2 \vec{V}, \tag{4}$$

where $[(\vec{\Omega} \times (\vec{\Omega} \times \vec{r})) + A_o]$ is a conservative force field and can be expressed by $\nabla\Phi \equiv (\vec{\Omega} \times (\vec{\Omega} \times \vec{r})) + A_o$, where Φ is a scalar function. Then Eq. (4) can be simplified as

$$\frac{D\vec{V}}{Dt} + 2(\vec{\Omega} \times \vec{V}) - \nabla\left(\frac{P}{\rho} + \Phi\right) + v\nabla^2 \vec{V}. \tag{5}$$

Taking curl in Eq. (5) yields

$$\frac{D\xi}{Dt} = (\xi \cdot \nabla)\vec{V} + v\nabla^2\xi - 2\nabla \times (\vec{\Omega} \times \vec{V}), \tag{6}$$

where the vorticity $\xi \equiv \nabla \times \vec{V}$.

Presume that, under hydrostatic state, $V = 0$, $P = P_o + P'$, and $\rho = \rho_o + \rho'$. The subscript o stands for the hydrostatic condition, the superscript $'$ is the variance of the disturbance. The relational expression $\rho = \rho_o[1 - \rho(T - T_o)]$ can be obtained by Boussinesq approximation. Substituting the relational expressions for P and ρ into Eq. (5) yields

$$\frac{D\vec{V}}{Dt} + 2(\vec{\Omega} \times \vec{V}) = -\frac{1}{\rho}\nabla P' + \beta(T - T_o)\nabla\Phi + v\nabla^2 \vec{V}, \tag{7}$$

and substituting Eq. (7) into Eq. (6) then results in

$$\underset{\text{(I)}}{\frac{D\xi}{Dt}} = \underset{\text{(II)}}{(\xi \cdot \nabla)\vec{V}} + \underset{\text{(III)}}{v\nabla^2\xi} + \underset{\text{(IV)}}{2(\Omega \cdot \nabla)\vec{V}} + \underset{\text{(V)}}{\nabla \times [\beta(T - T_o)\nabla\phi]}. \tag{8}$$

Equation (8) is the famous Helmholtz equation of hydrodynamics [11]. (I) stands for the acceleration term; (II) represents the vortex stretching term; (III) stands for the viscous diffusion term; and (IV) and (V) are vorticity generation terms generated by the Corolis force and the centrifugal force, respectively.

It can be found in Eq. (8) that within a heat rotary channel, the Corolis force and the centrifugal buoyant force effect play an important role in the flow field. The Corolis acceleration forms a couple of vortices normal to the main flow field, which help to enhance the mixing of the flow field and achieve a better heat transfer effect. The buoyant force effect occurs as the rotary cooling channel rotates at high speed and the temperature of the cooling liquid changes remarkably. It also interacts with the shaft position and the flow direction of the main flow field.

3 Experimental apparatus and procedures

3.1 Experimental apparatus

As shown in Fig. 1, the platform used in this experiment is specially designed for the test of adding transmission case oil containing nano particles into the oil duct of the RBC. Table 1

1. Tachometer
2. Motor
3. Inverter
4. Rotary blade coupling
5. Rear differential
6. Data recorder
7. Computer

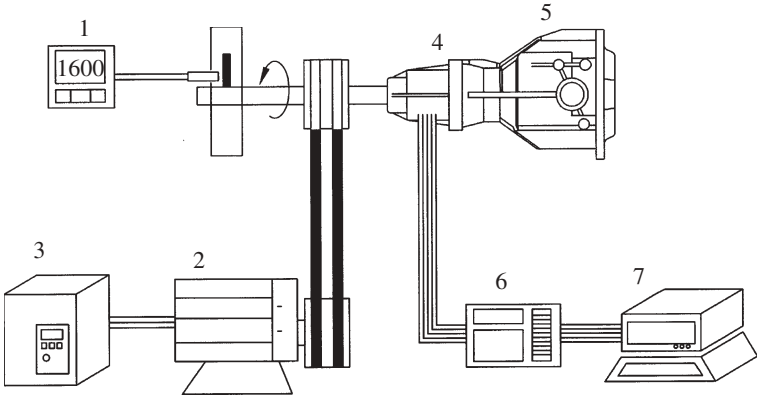

Fig. 1. Experimental setup

Table 1. Contents of nanofluids

Case	Particle	Concentration (wt%)
I	CuO	4.4 %
II	Al_2O_3	4.4 %
III	Antifoam	0.5 %

lists the composition of nano particles for various cases. The experimental system can be roughly divided into a testing section, the rotating main shaft and the data acquiring system.

The test section is the RBC of the central differential gear of *Tribute 3.0 L*, Mazda's latest real-time 4WD vehicle. Twelve temperature-measuring points are distributed evenly on the upper and lower (top and bottom) parts, respectively, along the testing section's axial direction, measuring the temperature distribution on the exterior top and bottom of the RBC. A photograph of the test section is shown in Fig. 2. For the radial direction, 12 points are selected every 30 degrees to measure the temperature distribution in the radial direction of the RBC. The temperature measured at each point is the local temperature of that part. The power of the rotating main shaft is supplied by a high-speed alternating current (AC) motor and the rotating speed is controlled by a frequency converter. This is to simulate the actual rotation. The system was driven by a five-HP high-speed AC motor (220 V, three-phase). Its maximum safe rotating speed is 3420 rpm. The rotating speed is read by a covered tachometer (KYODO DENKI ATAC-152 type). The drive of the high-speed motor is transmitted by a double-groove pulley and V-type belt.

The thermal elements are made of a blue wire (copper wire) and a red wire (constantan wire, 55%Cu, 45%Ni). The copper wire and the constantan wire must be welded and measured by an avometer to make sure that resistances of the thermal elements are identical. The thermal elements were placed on the exterior of the RBC and fixed with thermally conductive adhesive (OMEGA BOND 200 type).

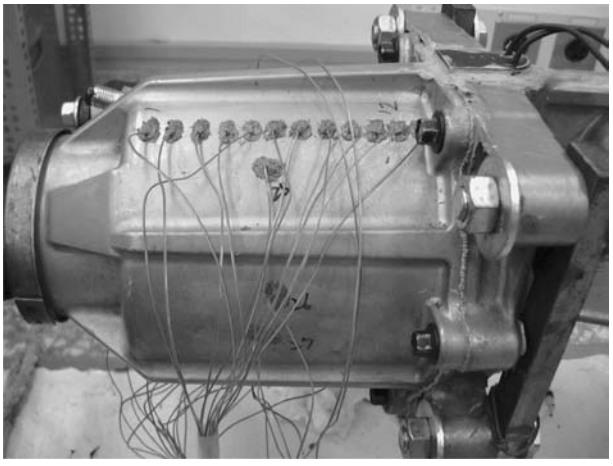

Fig. 2. Photograph of test section

The relationship between wall temperature and input power (q_{in}) by a direct current power supply must be established to evaluate the heat transfer value. Take a block of aluminum alloy with similar material and shape to those of the testing section. The ranges of voltage and current are 5.0 V–30.0 V and 0.27 A–1.54 A, respectively. The voltage and current values of each experiment can be used to estimate the input power. This test is performed in an insulated environment. After the temperature becomes stable, one corresponding temperature value is acquired. This way, the relationship between wall temperature and heat input can be established. The desired result of this experiment is a linear relational expression in the form:

$$q_{\text{in}} = 0.383T - 0.267. \tag{9}$$

3.2 Experimental procedures

Each component of the experimental apparatus is interrelated with the others, and a certain operational sequence should be obeyed to ensure the accuracy and the safety of persons involved. Therefore, the experimental procedures are laid out as follows:

(1) Add 40g nano particles with 860g engine oil to concoct the mixed liquid as a weight percentage concentration of 4.4%. Add this working liquid into the oil channel of the RBC.
(2) Make sure that the screws of each rotary component are fastened and each airproof component is well secured.
(3) Turn on the air conditioner and set the room temperature to 20°C. Turn on various instruments. Make sure that each of them can read relevant signals properly to prevent the occurrence of any erroneous message.
(4) Turn on the data recorder and make sure that the temperature reading at each temperature-measuring point is correct. Then start to monitor the temperature and set the timer to 60 minutes.
(5) Print out the temperatures at each temperature-measuring point. Then activate the frequency converter and adjust the rotating speed of the motor to the intended speed and turn on the timer simultaneously.
(6) Test operators should monitor the operation of the platform throughout the process and stop it immediately if any malfunction occurs.

(7) Print out the temperatures of each temperature-measuring point immediately as the test reaches 60 minutes at steady state.
(8) After printing, reduce the rotating speed to 200 rpm. Turn off the frequency converter and the motor when the temperature within the RBC drops.

3.3 Uncertainty analysis

In this experiment, Coleman and Steele [12] is referenced for the uncertainty analysis, with the data-reduction formula

$$R = f(x_1, x_2, x_3, \ldots, x_n), \tag{10}$$

where R are calculated parameters and x_n are measured parameters. Also, the uncertainty of the calculated parameters can be represented as

$$\delta R = \left[\sum_{k=1}^{n} \left(\frac{\partial R}{\partial X_k} \delta X_k \right)^2 \right]^{1/2}, \tag{11}$$

where $\delta X_k = \pm X_k$.

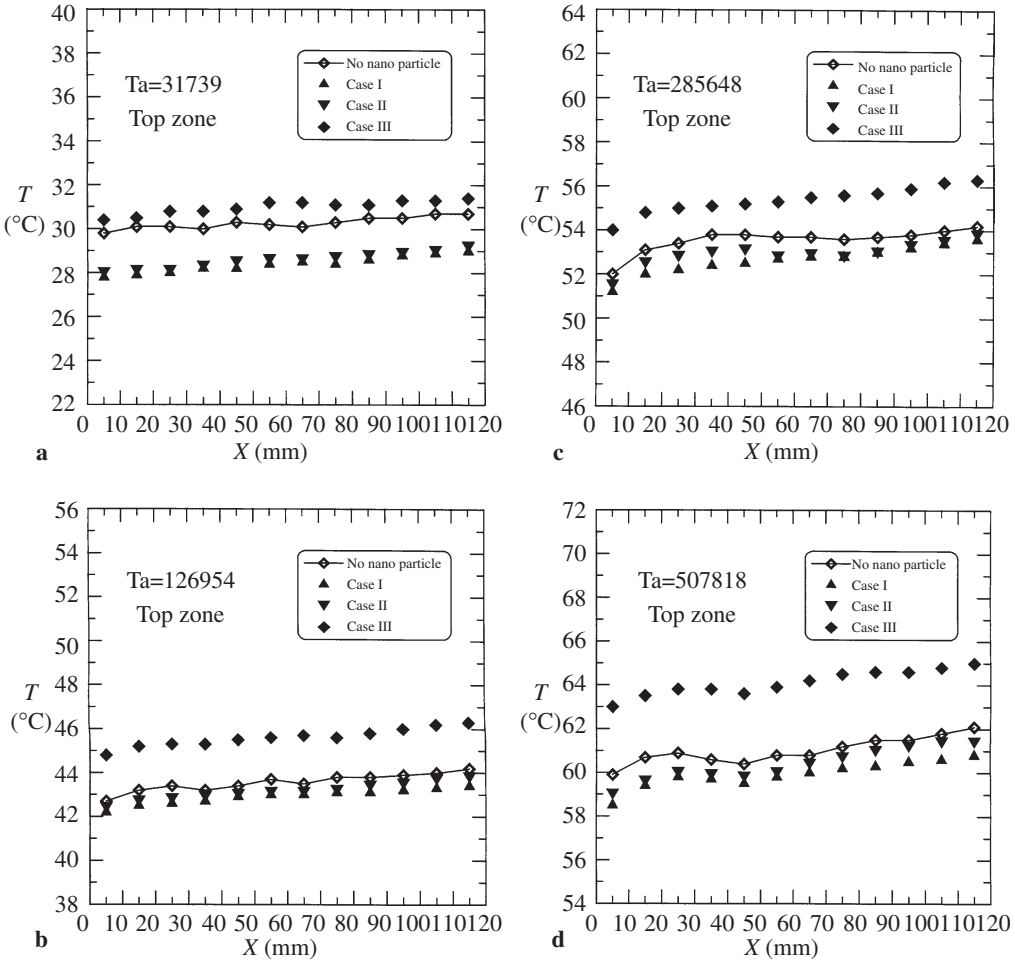

Fig. 3. Axial temperature distribution with various Taylor numbers at the top zone

The uncertainty of measured parameters and calculated parameters in the experimental procedure can be expressed as $R = R \pm \delta R$. Uncertainties in the Taylor number, temperature distribution and the Nusselt number were estimated as $\pm 1.86\%$, $\pm 3.21\%$ and $\pm 4.73\%$, respectively.

4 Results and discussion

Using automatic transmission oil without adding nano particles and three mixed liquids (Case I to Case III) at four different rotating speeds, this experiment measures the temperature distribution in radial and axial direction on the exterior surface of the RBC. Then the heat transfer performance of automatic transmission oil without nano particles is compared to that of two mixed cooling oils and cooling oil mixed only with antifoam. This is in an effort to find the desirable mixed liquid with the best heat transfer performance. To simulate the actual operation of a vehicle, the exterior temperature of the rotary blade coupling is measured as the rotating

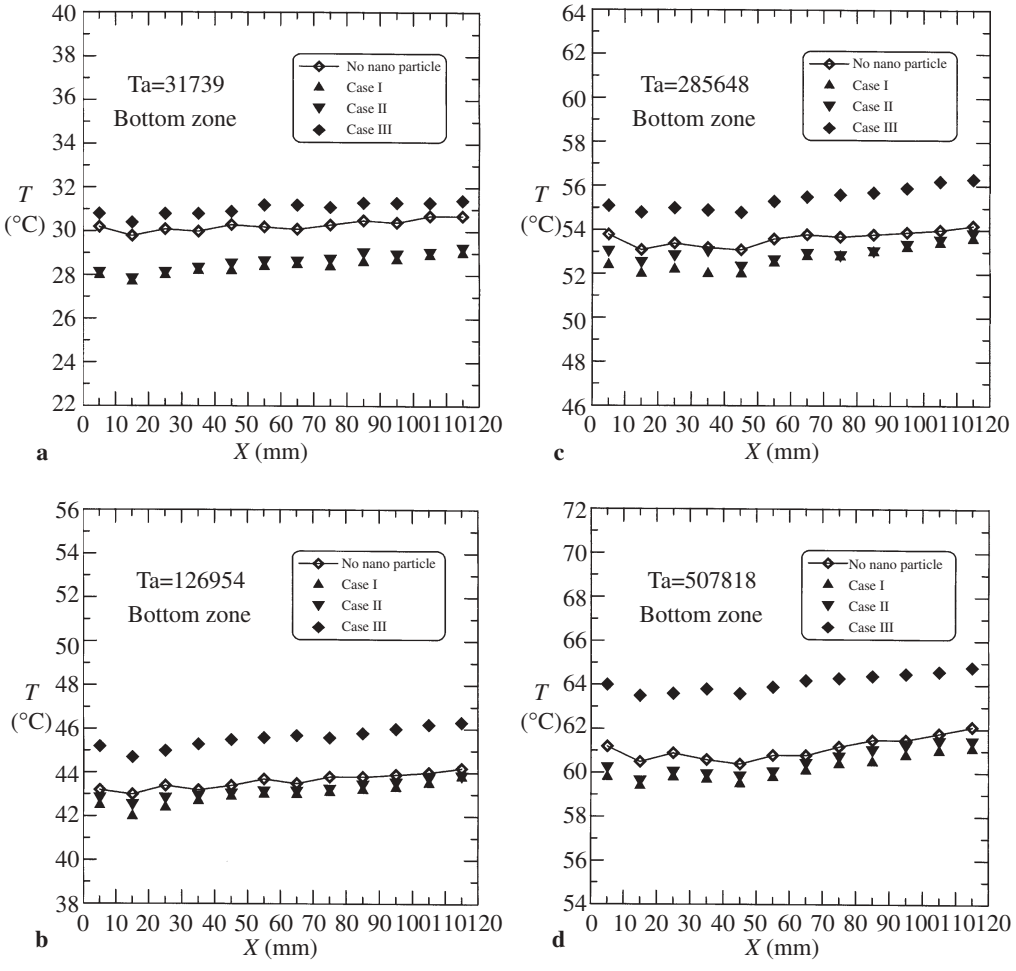

Fig. 4. Axial temperature distribution with various Taylor numbers at the bottom zone

speeds are at 400, 800, 1200 and 1600 rpm in an attempt to find the rotational speed effect. The analysis of the measured results is as follows.

The temperature distribution in Fig. 2 shows an alternating vibration phenomenon, which is closely related with the Taylor vortex in hydrodynamics. A Taylor vortex occurs within a small gap where the inner cylinder rotates while the outer cylinder remains at rest (this is similar to the operation of the RBC). Consequently, two vortex flows of opposite directions are produced. At the axial direction, the flows go toward and away from the interior wall of the RBC, which is called the secondary flow. As cooling oil flows to the interior wall of the RBC, the temperature drops because of the cooling effect of the liquid impact, while at the other direction, as the oil flows away from the interior wall, the cooling effect is less effective and the temperature of the component remains high. Accordingly, the temperature at the radial direction varies. The flow field in this case resembles that of the leading edge and trailing edge in a rotating channel. In this study, the secondary flow of the rotating flow field is produced by the Corolis force. The cooling effect on the trailing edge is better than that on the leading edge. This phenomenon is generated by the secondary flow pattern.

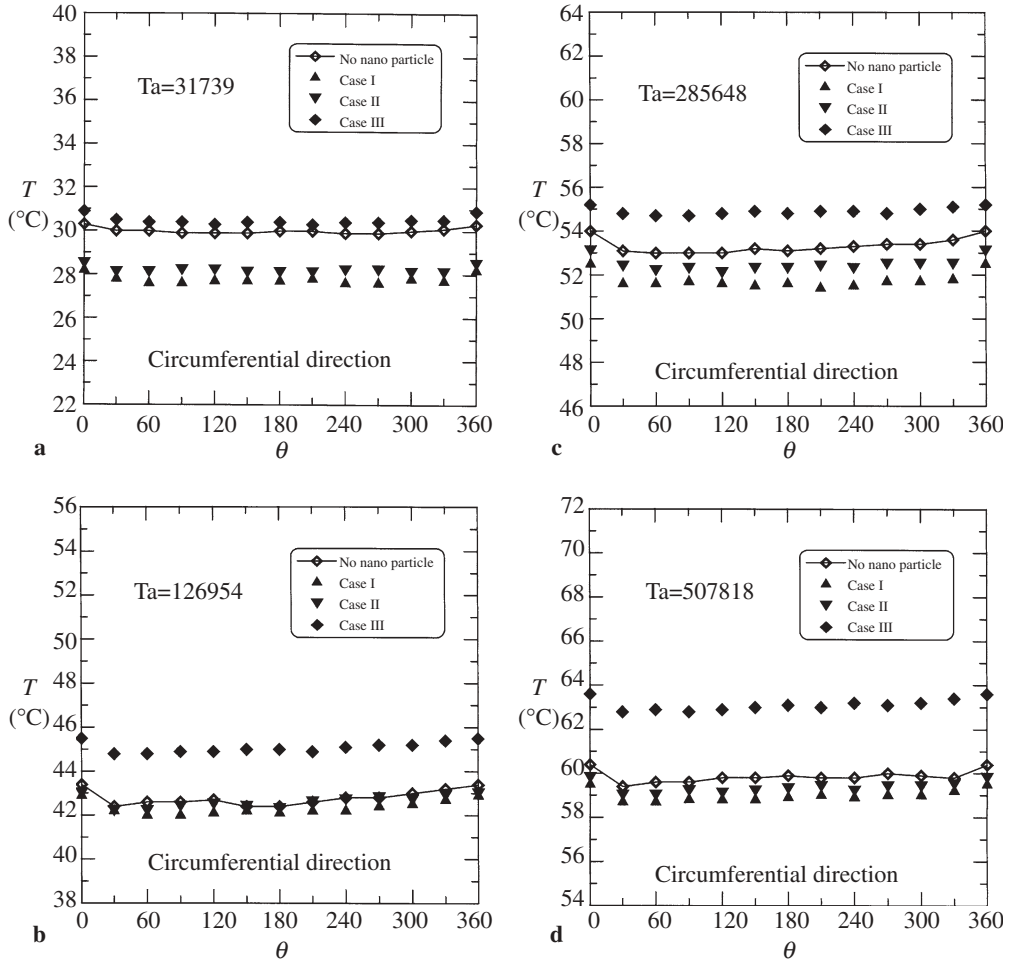

Fig. 5. Temperature distributions with various Taylor numbers at circumferential direction

A comparison between Fig. 3a–d finds that as the Taylor number increases (from Ta = 31739 to Ta = 507818), the top temperature also rises from 30°C to 60°C. It could be found that as the rotating speed increases onefold, the average temperature would rise about 10°C. Substitute this into Eq. (9) and the corresponding q_{in} and Nu values are acquired. The amplitude of temperature vibration generated by Taylor vortex also increases with the rise of the Ta value. This means that the temperature distribution is uneven and hot spots are apt to appear at high rotating speed operation. Hot spots tend to cause the concentration of heat stress at certain parts and affect the performance of the overall rotary blade coupling. Moreover, it is also found that the temperature rises at the axial direction because the rotary blade coupling is affected by the hotter differential gear at its back.

Comparing Case I and Case III in Fig. 3a–d, it is found that the lowest temperature belongs to oil with CuO nano particles (Case I), followed by that with Al_2O_3 (Case II) and oil without any addition. The highest temperature is obtained for oil with antifoam (Case III). Antifoam is added to prevent air from mixing with the engine oil as the blade rotates as it can help bubbles break or separate, decreasing the internal pressure of the rotating component. However, the heat transfer performance of the antifoam is bad enough to make the engine oil less capable of

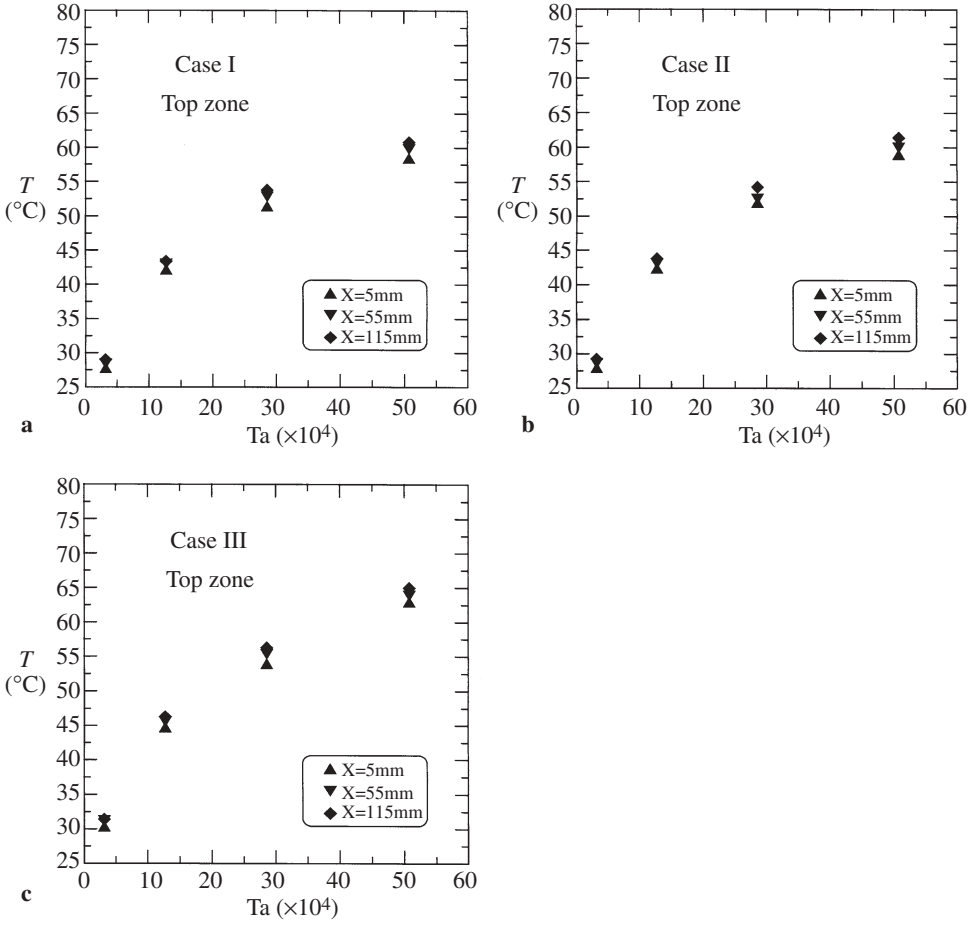

Fig. 6. Temperature distributions with various Taylor number at three different locations of the top zone

transfering heat. Taking the machine oil without any addition as the standard, it can be found that as Ta increases, the difference between Case I, Case II and oil without addition diminishes, which suggests that as the rotating speed increases, the heat transfer effect of the two kinds of nano particles decreases remarkably. As the Taylor number reaches a certain threshold value, the Taylor vortex effect that generates the vibrating temperature distribution is effectively contained by the increasing convection effect. The temperature difference of Case II and oil without addition also increases with the increase of the Taylor number.

Figure 4a–d shows the axial temperature distribution at the bottom part for various Taylor numbers. Figure 5a–d shows the radial temperature distribution for various Taylor numbers. The results are similar to those of Fig. 3a–d in terms of the rising extent of temperature at different Taylor numbers, the temperature sequence from Cass I to Case III, and the temperature rise caused by the differential gear behind the rotating shaft. At three different locations of the top zone along the axial direction (X = 5 mm, 55 mm and 115 mm), the temperature distributions in the case of Case I to Case III at different Taylor numbers are shown in Fig. 6a–c and calculated Nu values at X = 5 mm, 55 mm and 115 mm are shown in Fig. 7a–c. An effective empirical correlation can be established as follows:

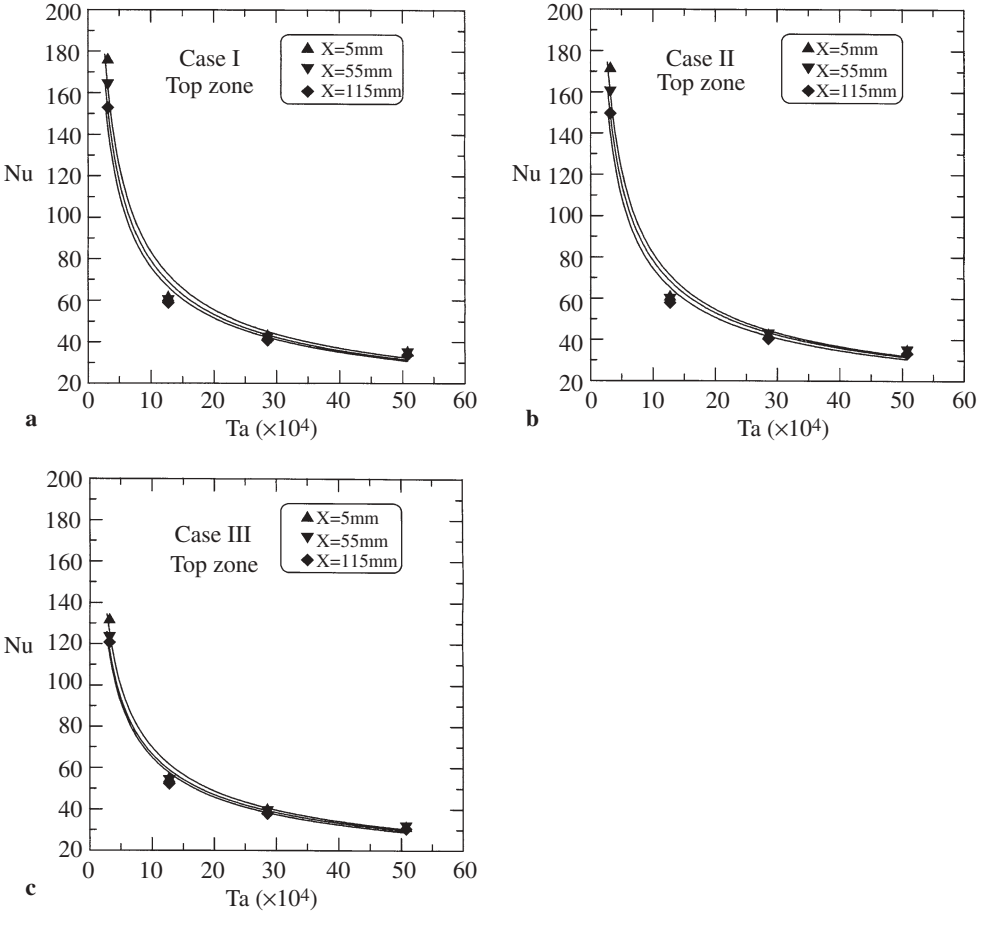

Fig. 7. Heat transfer distributions with various Taylor number at three different locations of the top zone

Table 2. The coefficents of the Nu vs. Ta correlation for various cases

X (mm)	Case I			Case II			Case III		
	C_1	C_2	δ (%)	C_1	C_2	δ (%)	C_1	C_2	δ (%)
5	318.22	−0.58	4.24	309.88	−0.58	3.94	227.04	−0.51	1.69
55	292.47	−0.57	3.69	283.84	−0.56	3.31	207.57	−0.50	1.40
115	270.85	−0.55	2.89	264.12	−0.55	2.83	204.19	−0.50	1.52

Empirical equation $\mathrm{Nu} = C_1\mathrm{Ta}^{C_2}$

$$\mathrm{Nu} = C_1\mathrm{Ta}^{C_2}. \tag{10}$$

This empirical equation can be provided as a reference to researchers on relevant issues. Relating corresponding coefficients and error values are listed in Table 2.

5 Conclusion

This study adds CuO and Al_2O_3 nano particles and antifoam, respectively, into automatic transmission oil. Then a comparison is made between their heat transfer performance and that of oil without adding such substances. The experiment measures the temperature distribution of the RBC exterior at four different rotating speeds (400 rpm, 800 rpm, 1200 rpm and 1600 rpm). The experimental results show that CuO has the lowest temperature distribution both at high and low rotating speed and accordingly the best heat transfer effect. Antifoam has the highest temperature distribution in the same conditions and accordingly the worst heat transfer effect. As the rotating speed increases, the Taylor vortex effect, which generates a vibrating temperature distribution, becomes less remarkable. This is because the increasing convection effect contains the Taylor vortex. Finally, an empirical correlation expression between the Ta number and the heat transfer coefficient was established, and it is helpful for the guiding reference of related automobile designers and researchers.

Acknowledgement

The authors would like to thank the National Science Council of the Republic of China for financially supporting this research under contract no. NSC 92-2212-E-270-004.

References

[1] Mazda Tribute: Training handout. MADZA Motor Corporation 2001.
[2] Tzeng, S. C.: The introduction and diagnostics of power transmission elements of 4WD vehicles. J. Mech. Industry **224**, 142–151 (2001) (in Chinese).
[3] Maxwell, C.: A treatise on electricity and magnetism, 2nd ed., pp. 435–441. Cambridge: Oxford University Press 1904.
[4] Liu, K. V., Choi, S. U. S., Kasza, K. E.: Measurements of pressure drop and heat transfer in turbulent pipe flows of particulate slurries. Argonne National Laboratory Report NL-88–15, 1998.
[5] Choi, S. U. S.: Enhancing thermal conductivity of fluids with nanoparticles. ASME paper FED231, 99–103 (1995).

[6] Eastman, J. A., Choi, S. U. S., Thompson, L. J., Lee, S.: Enhanced thermal conductivity through the development of nanofluids. In: Proc. Symp. on Nanophase and Nanocomposite Materials II (Komarneni, S., Parker, J. C., Wollenberger, H., eds.), pp. 3–11. Boston: Materials Research Society 1997.
[7] Lee, S., Choi, S. U. S., Li, S., Eastman, J. A.: Measuring thermal conductivity of fluids containing oxide nanoparticles. Trans. ASME J. Heat Transfer **121**, 280–289 (1999).
[8] Wang, X. W., Xu, X. F., Choi, S. U. S.: Thermal conductivity of nanoparticle-fluid mixture. J. Thermophys. Heat Transfer **13**, 474–480 (1999).
[9] Keblinski, P., Phillpot, S. R., Choi, S. U. S., Eastman, J. A.: Mechanisms of heat flow in suspensions of nano-sized particles (nanofluids). Int. J. Heat Mass Transfer **45**, 855–863 (2002).
[10] Li, J. F., Liao, H., Wang, X. Y., Normand, B., Ji, V., Ding, C. X., Coddet, C.: Improvement in wear resistance of plasma sprayed Yttria stabilized Zirconia coating using nanostructured powder. Tribology Int. **37**, 77–84 (2004).
[11] Morris, W. D.: Heat transfer and fluid flow in rotating coolant channels. Chichester: Wiley 1982.
[12] Coleman, H. W., Steele, W. G.: Experimentation and uncertainty analysis for engineers. New York: Wiley 1989.

Authors' addresses: S.-C. Tzeng and C.-W. Lin, Department of Mechanical Engineering, Chienkuo Technology University, 1 Cheih Shou N Rd., Chang Hua 500, Taiwan, R.O.C. (E-mail: tsc@ctu.edu.tw); K. D. Huang, Graduate Institute of Vehicular Engineering, Dayeh University, Chang Hua 500, Taiwan, R.O.C.